molecular pharmaceutics

ARTICLE

pubs.acs.org/molecularpharmaceutics

Characterization of CD44-Mediated Cancer Cell Uptake and Intracellular Distribution of Hyaluronan-Grafted Liposomes

Hussaini Syed Sha Qhattal and Xinli Liu*

Department of Pharmaceutical Sciences, School of Pharmacy, Texas Tech University Health Sciences Center, Amarillo, Texas 79106, United States

Supporting Information

ABSTRACT: Hyaluronan (HA) is a biocompatible and biodegradable linear polysaccharide which is of interest for tumor targeting through cell surface CD44 receptors. HA binds with high affinity to CD44 receptors, which are overexpressed in many tumors and involved in cancer metastasis. In the present study, we investigated the impact of HA molecular weight (MW), grafting density, and CD44 receptor density on endocytosis of HA-grafted liposomes (HA−liposomes) by cancer cells. Additionally, the intracellular localization of the HA−liposomes was determined. HAs of different MWs (5−8, 10−12, 175−350, and 1600 kDa) were conjugated to liposomes with varying degrees of grafting density. HA surface density was quantified using the hexadecyltrimethylammonium bromide turbidimetric method. Cellular uptake and subcellular localization of HA−liposomes were evaluated by flow cytometry and fluorescence microscopy. Mean particle sizes of HA−liposomes ranged from 120 to 180 nm and increased with increasing size of HA. HA−liposome uptake correlated with HA MW (5−8 < 10−12 < 175−350 kDa), grafting density, and CD44 receptor density and exceeded that obtained with unconjugated plain liposomes. HA−liposomes were taken up into cells via lipid raft-mediated endocytosis, which is both energy- and cholesterol-dependent. Once within cells, HA−liposomes localized primarily to endosomes and lysosomes. The results demonstrate that cellular targeting efficiency of HA−liposomes depends strongly upon HA MW, grafting density, and cell surface receptor CD44 density. The results support a role of HA−liposomes for targeted drug delivery.

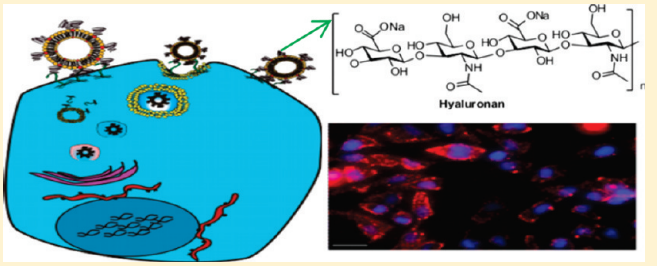

KEYWORDS: CD44, hyaluronan-grafted liposomes, tumor-targeted drug delivery, receptor-mediated cellular uptake, lipid raft-mediated endocytosis

INTRODUCTION

Nanoparticulate drug delivery systems (DDS) have shown great promise for delivery of diagnostic, therapeutic, and theranostic agents for a wide variety of human diseases, including cancer.[1] Advantages of nanoparticle (NP) over conventional drug delivery vehicles include better bioavailability, longer circulation time, and selective tumor distribution based upon the enhanced permeability and retention (EPR) effect of tumors.[2,3] Of the various NP systems tested, liposome-based NPs are among the best studied and clinically validated.[4] Surface-functionalized liposomes can be constructed to target diseased tissue and release drugs in a spatially and temporally controlled manner. Ligand-modified liposomes can also be created that bind preferentially to selective receptors on disease cells to improve drug targeting and therapeutic index.[5] However, for maximal success, it is critical to know the optimal ligand size and grafting density on the surface of the liposome and their effects on the uptake and cellular disposition of receptor-targeted liposomes.

CD44 receptor is a transmembrane glycoprotein (85 kDa) known to participate in a wide variety of cellular functions, including cell orientation, adhesion, migration, and matrix-cell signaling processes.[6] CD44 is overexpressed in many solid tumor cells including lung, breast, colorectal, gastric, pancreatic, renal, hepatocellular, and cervical cancer as well as melanoma.[7] Additionally, CD44 is a common marker for several cancer stem cells which exhibit highly malignant and chemoresistant properties.[8] The ligand for CD44 receptor is extracellular matrix hyaluronan (HA), which is a linear negatively charged polysaccharide formed by alternating D-glucuronic acid and *N*-acetyl-D-glucosamine. HA has been used as a drug carrier or targeting moiety for nanoparticles to target CD44-overexpressing cells.[9]

Natural HA is a hydrophilic, nonimmunogenic, biocompatible, and biodegradable polymer with a molecular weight of 10^6 to 10^7 Da; constituted by 2000−25,000 disaccharides under normal physiological conditions.[10,11] In addition to its principal receptor CD44, HA also interacts with several cell surface receptors, including RHAMM (receptor for hyaluronan-mediated motility, CD168), HARE (HA receptor for endocytosis), and Toll-like receptors-2 and -4.[12] RHAMM is important in regulating cell motility in wound healing and cancer.[13] HARE receptor is

Received: January 27, 2011
Accepted: June 22, 2011
Revised: June 11, 2011
Published: June 22, 2011

expressed in the sinusoidal endothelial cells of liver, spleen, and lymph nodes and acts as a scavenging receptor that clears hyaluronan and other glycosaminoglycans from the blood.[14] Toll-like receptors-2 and -4 mainly recognize hyaluronan oligomers in dendritic cells during inflammatory events.[15]

Natural high molecular weight HA (HMWHA) under certain pathological inflammatory conditions can be degraded by hyaluronidases to produce lower molecular weight HA fragments (LMWHA) and oligosaccharide HA (oligo HA, ~10−20 sugars in length) which are found in tissue injury and certain tumors.[16,17] HA of different MW forms bind to CD44 receptor but elicit different effects on cellular functions. For example, HMWHA is antiangiogenic, whereas LMWHA and oligo HA can induce angiogenic responses.[18,19] Similarly, high and low MW forms of HA provoke distinct anti-inflammatory and proinflammatory effects, respectively, upon binding to CD44.[20] Different molecular sizes of HA have differential effects on the rate of early wound contraction.[21] The MW of HA also significantly impacts its biodistribution,[22] cellular permeability,[23] and ligand−receptor interaction.[24] Consequently, the effect of HA MW should be investigated for any ligand-targeted DDS that uses HA as the targeting moiety.

HA has been coated on the liposome surface as a bioadhesive NP[25] or targeted NPs to deliver mitomycin C or doxorubicin to melanoma cells.[26,27] The HA coating provides a hydrophilic shield, similar to polyethylene glycol (PEG), for promotion of long blood circulation. Further, the addition of HA also provides targeting for CD44 positive cells. However, it remains unclear how HA size influences its targeting properties and how the surface HA ligand density affects the cellular internalization and intracellular trafficking of HA-grafted liposomes. Therefore, the aims of the current study were to delineate the influences of HA molecular weight and grafting density, as well as cellular CD44 receptor expression level, on the cellular uptake of HA−liposomes and to determine the intracellular localization of HA−liposomes.

EXPERIMENTAL SECTION

Chemicals. L-α-Phosphatidylcholine, egg, chicken (Egg PC), 1,2-dioleoyl-*sn*-glycero-3-phosphoethanolamine (DOPE), lissamine rhodamine PE (Rh-PE), and cholesterol were purchased from Avanti Polar Lipids (Alabaster, AL). Hyaluronan of various MWs (5−8, 10−12, and 175−350 kDa) was purchased from Lifecore Biomedical (Chaska, MN). High MW hyaluronan (HMWHA, 1600 kDa, sodium salt from *Streptococcus equi*), hexadecyltrimethylammonium bromide (CTAB), 1-ethyl-3-(3-dimethylaminopropyl)carbodiimide (EDC), *N*-hydroxysulfosuccinamide (NHSS), chlorpromazine, amiloride, methyl-β-cyclodextrin, filipin III, nystatin, and Nile Red were purchased from Sigma-Aldrich (St. Louis, MO). Sodium acetate and phosphate-buffered saline (PBS) were purchased from Fisher Scientific (Pittsburgh, PA). DAPI (4,6-diamidino-2-phenylindole), LysoTracker Green (DND-26), and Texas Red dextran (MW 3 kDa) were purchased from Invitrogen (Carlsbad, CA). Fluorescein-labeled hyaluronans of various MWs (FL-HA) were synthesized based on a published method,[28] and the degree of substitution of fluorescein was determined by fluorescence intensity analysis using fluorescein sodium as standard (Supporting Information). Texas Red labeled 5−8 kDa hyaluronan (TR-HA) was made according to a published method.[29] All other chemicals were purchased from Sigma-Aldrich and were of standard analytic grade or higher.

Cell Culture. Human lung carcinoma epithelial cell line A549 and human breast cancer cell lines MDA-MB-231 and MCF7 were obtained from ATCC (Manassas, VA). A549 cells were maintained in RPMI-1640 medium (Mediatech, Inc.; Manassas, VA) supplemented with 10% fetal bovine serum (FBS) (Gibco, Invitrogen). MDA-MB-231 and MCF7 cells were cultured in RPMI-1640 medium with 10% FBS, 100 U/mL penicillin, and 100 μg/mL streptomycin and incubated at 37 °C in a humidified atmosphere with 5% CO_2.

Hyaluronan-Conjugated Liposome Preparation and Characterization. Plain (unsubstituted) liposomes were prepared by thin lipid film hydration and extrusion method. Briefly, a homogeneous chloroform solution of the lipid components (PC:PE:Chol in 65:5:30 molar ratios) was evaporated and the resulting lipid film was dried under vacuum overnight. Films were hydrated in phosphate buffered saline (PBS) with an initial total lipid concentration of 5−10 mM. The suspension was bath-sonicated for 30 min, followed by extrusion through stacked 100 nm pore size polycarbonate membranes (Nucleopore, Whatman Inc., Piscataway, NJ) using a hand-held extruder (Avestin Inc., Ottawa, ON, Canada).

To prepare HA-conjugated liposomes (HA−liposome), we used a method similar to that reported by Yerushalmi et al.,[25] where different MWs of HA were hydrated in water (pH 4.0) overnight to allow swelling and complete solubilization. After the addition of the coupling agents EDC and NHSS to activate HA, the pH of the solution was back-titrated to 4.0 using 1 M HCl. The solution was then incubated for an additional 2 h at 37 °C before being transferred to 1 mL of PE-containing plain liposome suspension (pH 8.6) for overnight stirring at 37 °C. The excess reagents and free HA were removed as the supernatant after three cycles of ultracentrifugation at 150000*g*. Rhodamine labeled PE (Rh-PE) at 0.5 mol % was used as the fluorescent lipid in formulations prepared for the fluorescence microscopy studies. Fluorescent dye Nile Red at 1 mol % served as a fluorescence probe in liposome formulations used in flow cytometry studies. Nile Red loaded liposomes were subjected to low velocity centrifugation and gel filtration on a Sephadex G-25 column to separate unentrapped Nile Red. After separation, all Nile Red liposomes were used immediately for cellular uptake assays. Less than 5% free dye released from formulations after 2 h incubation in medium determined by equilibrium dialysis. The liposome particle size, zeta potential, and polydispersity were measured by dynamic light scattering analysis of dilute samples using a Nicomp 380/ZLS particle sizing analyzer (Santa Barbara, CA).

Determination of the Concentration of Hyaluronan. The amount of unconjugated (free) HA in the supernatants after ultracentrifugation was quantified using the published hexadecyltrimethylammonium bromide (CTAB) turbidimetric method with modification.[30] Briefly, 50 μL of HA standard solutions (0.1−2 mg/mL) or diluted supernatants were added to a 96-well plate. The samples were incubated with 50 μL of 0.2 M sodium acetate buffer for 10 min at 37 °C. Then, 100 μL of 10 mM CTAB solution was added to the mixture, and the absorbance of the precipitated complex was read within 10 min against the blank at 570 nm using a microplate reader (BioTek Instruments, Inc., Winooski, VT). The amount of conjugated HA was calculated by subtracting the amount in the supernatant fraction from the initial amount added to the reaction mixture.

Receptor Expression Analysis. CD44 expression levels were determined by combined flow cytometry, immunocytostaining, and Western blot analysis. For flow cytometry analysis, 0.5×10^6 cells were incubated with the fluorescein isothiocyanate (FITC)-conjugated mouse anti-human CD44 monoclonal antibody (BD Pharmingen, San Diego, CA) for 30 min at 4 °C. FITC mouse IgG_{2b} κ antibody was used as isotype control. Cells also were incubated with 50 μg/mL of FL-HMWHA in PBS at 4 °C for 30 min, washed three times with ice cold PBS, and resuspended in 0.4 mL PBS. The fluorescence intensity was analyzed using flow cytometry as described below. For immunocytostaining, exponentially growing cells were plated on sterile coverslips (12 mm) placed in a 12-well plate at a density of 50,000 cells per well, and cells were allowed to attach overnight. The cells were then washed three times with PBS, followed by fixation with an ice cold acetone:methanol mixture (50:50 v/v) for 5 min. Fixed cells were stained using anti-human CD44H (clone 2C5, R&D Systems) as primary antibody and Alexa Fluor 546 labeled goat anti-human antibody (Invitrogen) as secondary antibody. Cells were counterstained with 2 μg/mL DAPI for nuclear recognition prior to imaging on the fluorescent microscope. For Western blot analysis, cells were lysed at 4 °C in RIPA buffer. Proteins extracted from cells were resolved by SDS−PAGE, electrophoretically transferred onto polyvinylidene membrane, and probed with CD44H antibody (R&D Systems). β-Actin antibody was used for equal loading control. Specific proteins were visualized with enhanced chemiluminescence detection reagent (Amersham Pharmacia). For cell surface RHAMM (CD168) receptor staining, cells were incubated with mouse anti-human monoclonal CD168 antibody (Abcam) or isotype control (IgG1) for 30 min at 4 °C. Cells were washed and incubated with a goat anti-mouse IgG Alexa Fluor 488-conjugated antibody for 45 min at 4 °C. Cells were then washed and resuspended in the FACS buffer and analyzed by flow cytometer.

Cellular Uptake Studies. Various HA−liposomes carrying different amounts of low (5−8 and 10−12 kDa) and high (175−350 and 1600 kDa) molecular weight HA were prepared as described above. The cellular uptake of the formulations was then studied using tumor cell lines with different levels of CD44 receptor density with the aid of fluorescence microscopy (Rh-PE liposomes) and flow cytometry (Nile Red loaded liposomes). Briefly, $0.2-0.3 \times 10^6$ cells per well were plated in a 12-well plate and allowed to attach overnight. The complete growth medium was replaced with the serum- and antibiotic-free medium containing Rh-PE labeled plain liposomes or various HA−liposomes at a final total lipid concentration of 100 μM. Lipid concentration was determined spectrophotometrically at 560 nm based on Rh-PE lipid standards. The cells were incubated for 2 h at 37 °C, and nucleus dye DAPI (2 μg/mL) was added 20 min before cells were visualized using fluorescence microscopy. For quantitative analysis, cells were incubated with Nile Red loaded plain liposomes or various HA−liposomes in serum- and antibiotic-free medium with a final Nile Red concentration of 0.5 μM. After 2 h of incubation, the cells were washed three times with ice cold PBS, then harvested and analyzed by flow cytometer. Cells incubated in media alone without any formulations served as the negative control for autofluorescence. To test whether the HA−liposome uptake was mediated by CD44 receptor, the cells were pretreated with 10 mg/mL free HA polymer (175−350 kDa, hydrated overnight in serum- and antibiotic-free medium) for 1 h before addition of Rh-PE labeled or Nile Red labeled plain liposomes or various HA−liposomes for an additional 2 h.

Fluorescence Microscopy. The localization of various fluorophores in cells was investigated with an Olympus IX81 inverted fluorescence microscope. Excitation and emission filters were, respectively, 360 ± 20 nm and 460 ± 25 nm for blue channel (DAPI), 470 ± 40 nm and 525 ± 50 nm for green channel (LysoTracker), and 560 ± 55 nm and 645 ± 75 nm for red channel (Rh-PE). Images were captured with a Hamamatsu CCD camera using a constant exposure time (25 ms for blue channel, and 100 ms for red channel). Fluorescence images were viewed using Slidebook 5.0 software (Olympus Inc., Center Valley, PA) in blue and red channels to visualize the presence of cells (DAPI, blue) and liposomes (Rh-PE, red) and in green channel to visualize the LysoTracker probe, and the overlay was used to show the cellular association of liposomes.

Flow Cytometry. A FACScan flow cytometer (BD Biosciences, San Jose, CA) equipped with a 488 nm laser was used to analyze Nile Red labeled liposomes (lipid-bound dye $\lambda_{ex\text{-}max}$ = 550 nm, $\lambda_{em\text{-}max}$ = 636 nm). At least 10,000 cells were analyzed for each experiment. The flow cytometric data were presented as frequency distribution histograms. The uptake of control liposomes was set as 100%, and the relative uptake of different treatments was presented as percentage of control. For the cells pretreated with different endocytic inhibitors, the mean cell fluorescence was normalized to that of the untreated cells. All experiments were repeated at least three times.

Endocytosis Inhibition. The effect of temperature on HA−liposome uptake was studied by incubating the A549 cells with the Nile Red containing HA−liposomes for 2 h at 4 °C. The effects of several membrane entry inhibitors on the uptake of HA−liposomes were examined by preincubating the A549 cells with serum-free medium containing chlorpromazine (10 μg/mL), amiloride (25 μg/mL), methyl-β-cyclodextrin (5 mM), filipin III (5 μg/mL), or nystatin (25 μg/mL) for 1 h at 37 °C, and then treating the cells with various Nile Red loaded HA−liposomes or FL-HMWHA for an additional two hours.[31] The concentrations of inhibitors were based on the literature[32,33] and were not cytotoxic. At the end of incubation, the adherent cells were washed twice with ice cold PBS and then trypsinized for a prolonged period of time (6 min) to dissociate the surface bound formulation.[34] Internalized HA−liposomes were quantified by flow cytometry.

Intracellular Localization. A549 cells were treated with Rh-PE labeled liposomes for 2 h. The cells were then washed three times with PBS, followed by incubation with LysoTracker Green (150 nM for 5 min) and DAPI (2 μg/mL). The cells treated with Texas Red conjugated 5−8 kDa HA (600 μg/mL for 2 h) and Texas Red dextran (3 kDa, 500 μg/mL for 2 h) were used as controls. The stained cells were observed under the Olympus IX81 fluorescence microscope.

Statistical Analysis. Values are expressed as mean ± SEM unless stated otherwise. All statistical analysis was done using GraphPad Prism 5 software (San Diego, CA, USA). Differences between two means were tested using an unpaired, two-sided Student's *t*-test. Multiple group comparisons were performed by one-way ANOVA followed by Bonferroni's posttest analysis. Differences with $p < 0.05$ were considered significant.

RESULTS

CD44 Receptor Expression. We first used a combined method of flow cytometry, immunocytostaining, and Western blot analysis to quantitatively determine the relative surface expression levels of CD44 receptors in tumor cell lines. For flow

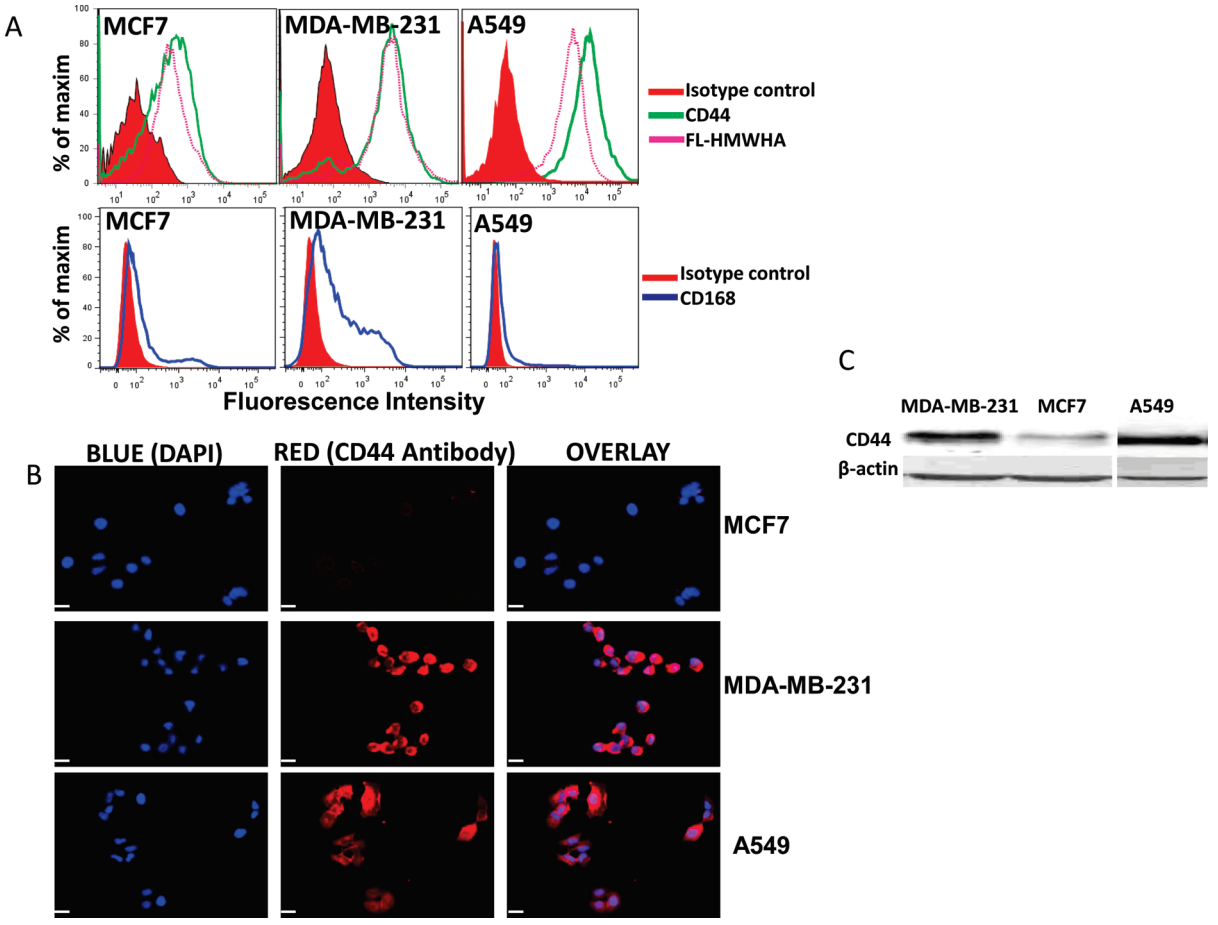

Figure 1. CD44 and CD168 expressions in different cell lines. (A) Flow cytometry histograms display cellular binding to FITC-IgG_{2b} isotype control (red filled curve), FITC-CD44 antibody (green curve), and fluorescein-labeled HMWHA (FL-HMWHA, broken pink curve) (top panel), and cellular binding to CD168 antibody (blue curve, bottom panel). (B) Immunocytostaining of CD44 in MCF7 (top), MDA-MB-231 (middle), and A549 cells (bottom). The blue channel shows the DAPI stained nuclei, the red channel displays binding to anti-CD44 antibody, and the overlay represents the cellular localization of CD44 receptor. Images are at 200× magnification, and scale bar is 25 μm. (C) Western blot analysis of CD44 expressions in different cell lines.

cytometry, human breast cancer cell lines MCF7 and MDA-MB-231 and human lung cancer cell line A549 were directly stained with FITC-CD44 antibody (recognizes all CD44 isoforms). As shown in Figure 1A, all the tested cells showed higher binding to FITC-CD44 antibody than the isotype control, indicating the presence of CD44 receptors in these cells. However, the binding of FITC-CD44 antibody to the MCF7 cells was much lower than that of the MDA-MB-231 and A549 cells, suggesting relatively higher expressions of CD44 receptors in the MDA-MB-231 and A549 cells. The CD44 receptors are capable of binding to its endogenous ligand HMWHA, evidenced by the shift of the fluorescence peak to higher intensity upon staining the cells with fluorescein-labeled HA (FL-HMWHA, 1600 kDa). The CD44 receptor expressions also were visualized using immunocytostaining. Very little red fluorescence (representative of binding of anti-CD44 antibody) was associated with MCF7 cells compared to MDA-MB-231 and A549 cells, which displayed a strong staining for this adhesion molecule CD44 (Figure 1B). Western blot analysis of whole cell lysate further confirmed the relatively low expression of CD44 in MCF7 cells, and high expression in A549 and MDA-MB-231 cells (Figure 1C). Because RHAMM (CD168) receptor is also implicated in cancer, we studied the surface expression of CD168 in the same cells. Flow cytometry results showed weak expression of CD168 in MDA-MB-231 cells and almost no surface expression in MCF7 and A549 cells (Figure 1A). Therefore, we focused on CD44 as principal hyaluronan receptor in the following study.

HA−Liposome Characterization. The reasons for making hydrophilic HA-functionalized liposomes are to improve the "stealth" properties of liposomes and to provide CD44 receptor-mediated active tumor targeting. Hyaluronan-conjugated liposomes (HA−liposomes) were obtained by covalent linkage of the glucuronic acid moiety of the targeting ligand HA to the primary amine of DOPE of the preformed liposomes using EDC/NHSS coupling chemistry. As shown in Figure 2A, the HA−liposomes displayed negative zeta potentials, indicating successful conjugation because HA is polyanionic at physiological pH. The particle sizes of the plain liposomes and HA−liposomes ranged from 120 to 180 nm. There was a trend toward an increase in the particle size of HA−liposomes as the MW of HA increased from 5−8 kDa to 1600 kDa. The polydispersity index of HA−liposomes was below 0.3 for all the formulations, indicating limited variation in particle size. However, the 1600 kDa HA−liposomes consistently showed higher polydispersity index from batch to batch, likely due to the highly polydisperse nature of HMWHA.

A

Liposomes	Particle Size (nm)	PDI	Zeta Potential (mv)	HA (mg) Grafted	HA: Lipid (μg HA / μmol Lipid)
Plain	126±3	0.159	0±4.1	NA	NA
5-8kHA	130±1	0.206	-2.16±0.8	1.48	304
10-12kHA	151±6	0.278	-2.20±7.6	1.52	267
175-350kHA	165±32	0.208	-5.76±2.6	1.36	341
1600kHA	178±55	0.289	-17.5±6.2	1.52	613

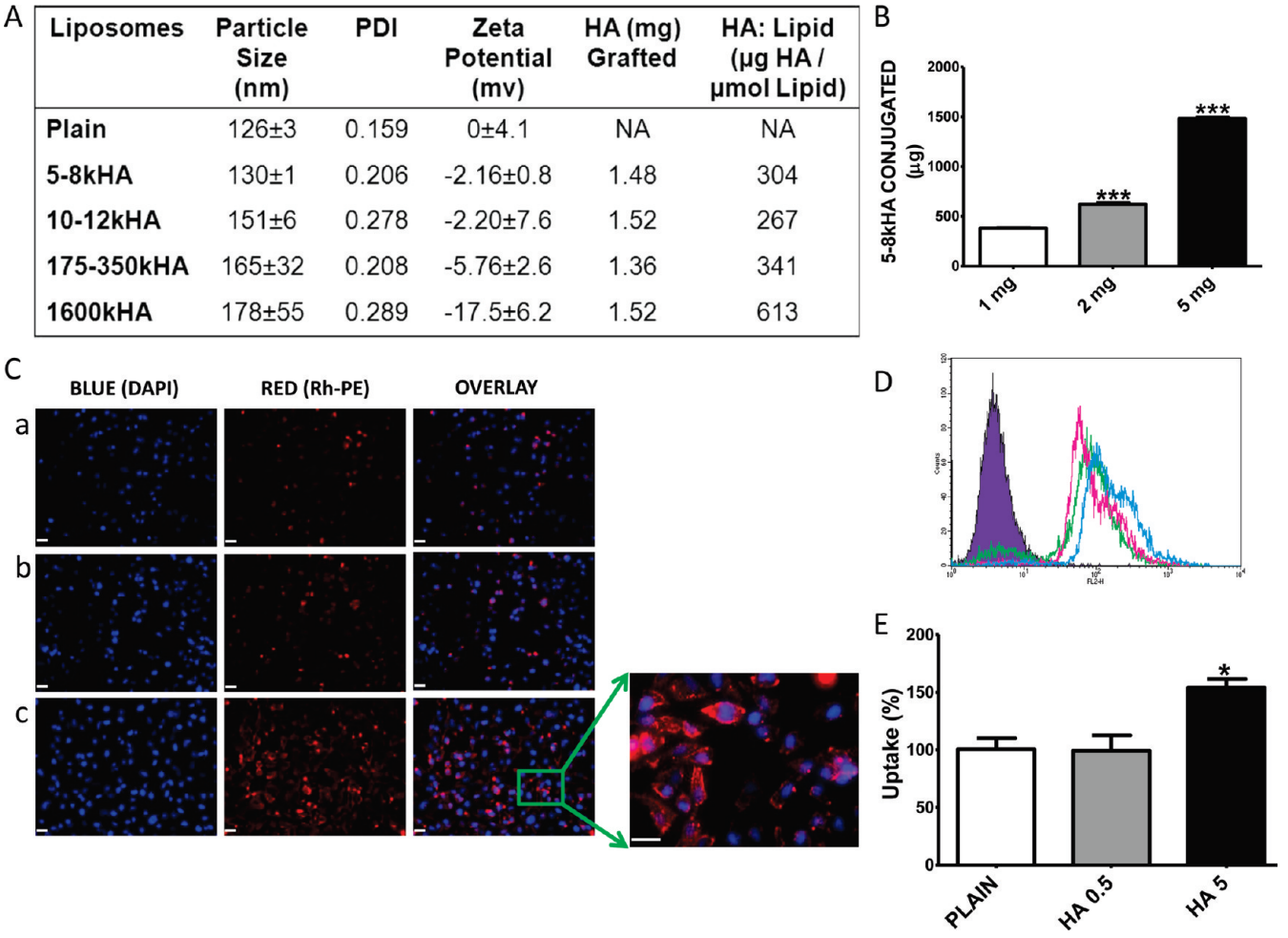

Figure 2. (A) Physical characteristics of HA−liposomes detailing composition, particle size, polydispersity index (PDI), zeta potential, and HA:lipid ratio. The size and charge represent mean ± SD, n = 3. (B) Quantitation of the degree of HA conjugation by CTAB turbidimetric method after conjugating 1, 2, and 5 mg of 5−8 kDa HA to the preformed liposomes. (C) Fluorescence microscopy images showing A549 cellular uptake of plain liposomes (a), 5−8 kDa HA−liposomes with low grafting density (b), and 5−8 kDa HA−liposomes with high grafting density (c). The blue channel shows DAPI stained nuclei, the red channel displays the Rh-PE labeled liposomes, and the overlay represents cellular association of liposomes. Images are at 200× magnification, and scale bar is 25 μm. Magnified image was at 400× magnification. (D) The flow cytometry histogram displays the relative fluorescence intensity of unstained control A549 cells (filled curve) or cells treated with Nile Red loaded plain liposomes (green curve), or 5−8 kDa HA−liposomes with low (∼0.2 mg HA, red curve) and high HA grafting densities (∼1.5 mg HA, blue curve). (E) The quantitative analysis of percentage of cellular uptake of Nile Red labeled HA−liposomes in comparison to plain liposomes. The bars represent mean ± SEM of each treatment, n = 3, * represents $p < 0.05$ after one-way ANOVA, followed by Bonferroni's multiple comparison tests.

The HA ligand density on the surface of liposomes can potentially affect its cellular binding and molecular targeting. To precisely measure and control the ligand density, we analyzed the HA concentration using the CTAB turbidimetric method. CTAB is a cationic surfactant that readily precipitates the polyanionic HA to form a complex with strong light absorption at 570 nm. When the initial amount of HA (5−8 kDa) added to the liposome mixture increased from 1 to 5 mg, the amount of HA conjugated to the liposomes increased proportionally from 0.38 to 1.48 mg (Figure 2B). Further addition of HA did not dramatically improve the surface coverage of HA, but increased the viscosities of the particles, especially for the highly viscous and elastic HMWHA (1600 kDa) (data not shown). Thus, we used 5 mg of various sizes of HA as the starting material to make all the HA−liposomes with the HA to lipids ratio (μg HA/μmol lipids) ranging from 267 to 613 μg/μmol (Figure 2A).

Effect of HA Grafting Density on Cellular Uptake of HA−Liposomes. To determine whether an optimal HA ligand density for maximal tumor cell targeting exists, the cellular uptakes of HA−liposomes with different HA ligand densities were visualized and quantified using fluorescence microscopy (Rh-PE labeled HA−liposomes) and flow cytometry (Nile Red loaded HA−liposomes), respectively. Rh-PE is a fluorescent rhodamine labeled lipid that is part of liposome components and displays red fluorescence. Nile Red is a lipophilic fluorescent dye that mainly partitions into the liposome bilayers and can be excited with 488 nm laser. We controlled the density of HA ligand coated onto the liposome surface by the addition of 0.5 and 5 mg of 5−8 kDa HA for the coupling reaction, which resulted in the final HA conjugation of approximately 0.2 and 1.5 mg, respectively. We studied the cellular uptake of these 5−8 kDa HA−liposomes with two HA grafting densities in comparison to plain liposomes. As shown in Figure 2C, cellular

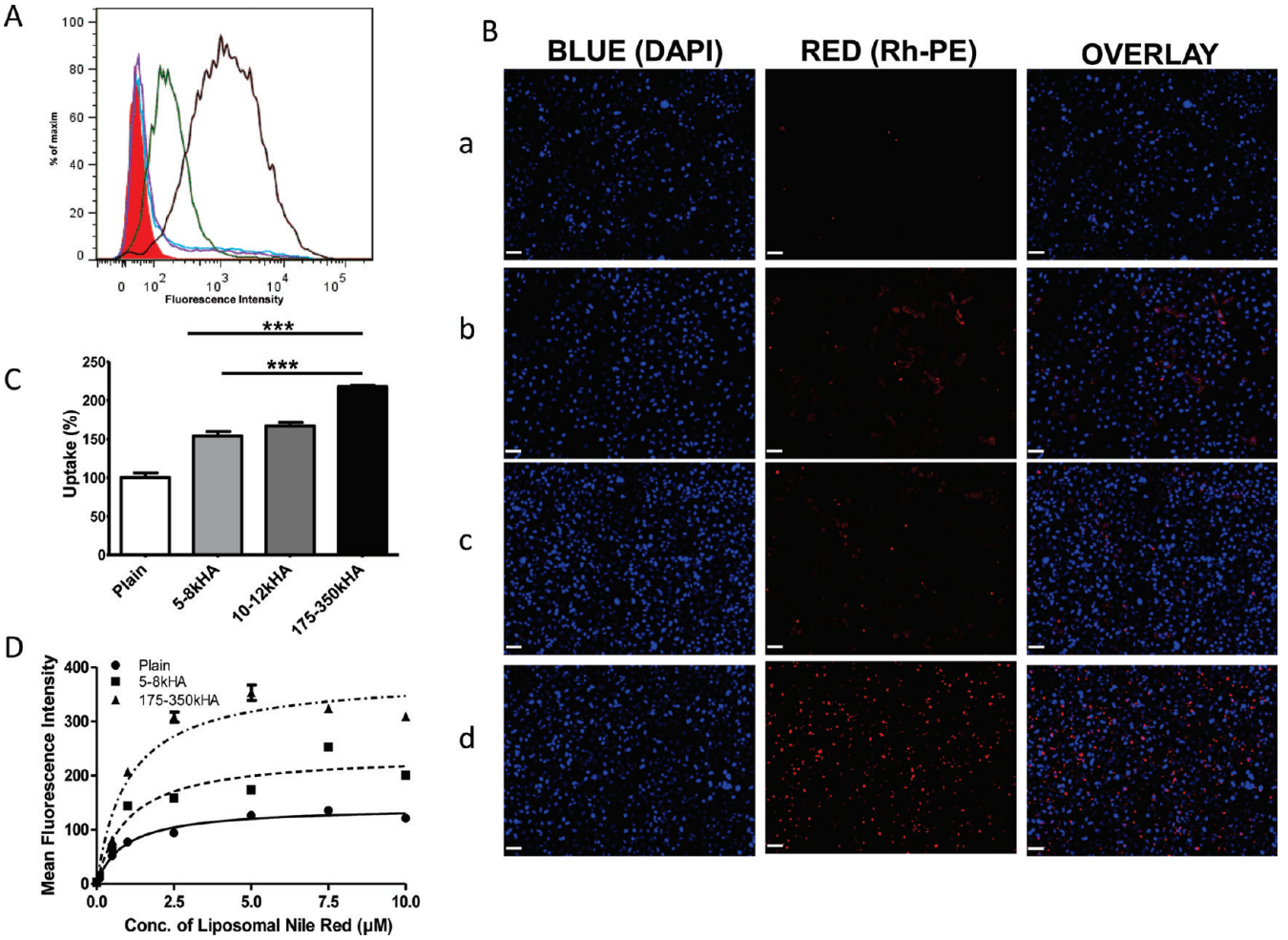

Figure 3. Effect of HA molecular weight on cellular uptake of HA−liposomes in A549 cells. (A) Flow cytometry histogram shows A549 cells stained with FL-HA of different molecular weights [no HA (red filled curve), 5−8 kDa HA (blue curve), 10−12 kDa HA (purple curve), 175−350 kDa (green curve), and 1600 kDa (black curve)]. (B) Fluorescence microscopy images display cellular association and uptake of Rh-PE labeled plain (a), 5−8 kDa HA−liposomes (b), 10−12 kDa HA−liposomes (c), and 175−350 kDa HA−liposomes (d). Blue channel shows DAPI stained nuclei, red channel displays the Rh-PE labeled liposomes, and the overlay represents cellular association of liposomes. Images are at 100× magnification, and scale bar is 50 μm. (C) The quantitative analysis of percentage of cellular uptake of Nile Red labeled different molecular weights of HA−liposomes. The bars represent mean ± SEM of each treatment, $n = 6$, *** represents $p < 0.0001$ after one-way ANOVA followed by Bonferroni's multiple comparison tests. (D) Concentration dependent binding and internalization of Nile Red loaded plain liposome (●), 5−8 kDa HA−liposomes (■), and 175−350 kDa HA−liposomes (▲) in A549 cells.

uptake of the Rh-PE labeled plain liposomes was similar to that of the 5−8 kDa HA−liposome with the low grafting density, as demonstrated by similar red fluorescence in the cells exposed to these two formulations. In contrast, cells treated with the HA−liposomes with the high grafting density (1.5 mg of surface anchored HA) showed significantly higher red fluorescence associated with cells. These qualitative results were confirmed by quantitative flow cytometric analysis using Nile Red loaded 5−8 kDa HA−liposomes. The mean fluorescence uptake of HA−liposomes with 1.5 mg of surface HA was significantly higher than that of the plain liposomes and HA−liposomes with only 0.2 mg of surface HA ($p < 0.05$, one way ANOVA, Figures 2D, 2E). This finding suggests that a critical density of the ligand is required on the surface of the liposomes to bind to CD44 receptor effectively.

Effect of HA Molecular Weight on the Cellular Uptake of HA−Liposomes. To study the effect of size of HA ligand on the efficacy of targeted delivery, we first analyzed the binding affinity of fluorescein-labeled HA (FL-HA) of defined molecular sizes to cells of varying levels of CD44 receptor using flow cytometry. FL-HA has proven to be a sensitive and specific probe for testing HA binding function of CD44.[35,36] Measurement of the fluorescence intensity of FL-HA indicated the HA disaccharide-to-fluorescein molar ratios were approximately 21, 23, 27, and 26, for 5−8 kDa, 10−12 kDa, 175−350 kDa, and 1600 kDa FL-HA, respectively. Figure 3A showed an increase in binding to A549 cells with increasing molecular size of FL-HA (5−8 ≈ 10−12 < 175−350 < 1600 kDa). We observed similar patterns in MCF7 and MDA-MB-231 cells (Figure S1 in the Supporting Information). Next, we prepared a series of liposomes functionalized with different MWs of HA [5−8, 10−12, and 175−350 kDa, with high grafting density (∼ 1.5 mg HA)] and evaluated their cellular internalization. The 1600 kDa HA was not included due to its high polydispersity, high viscosity, and difficulty to remove unconjugated HMWHA. Fluorescence microscopy data showed that increasing the size of HA led to an increased A549 cellular uptake of Rh-PE labeled HA−liposomes (Figure 3B). This trend was

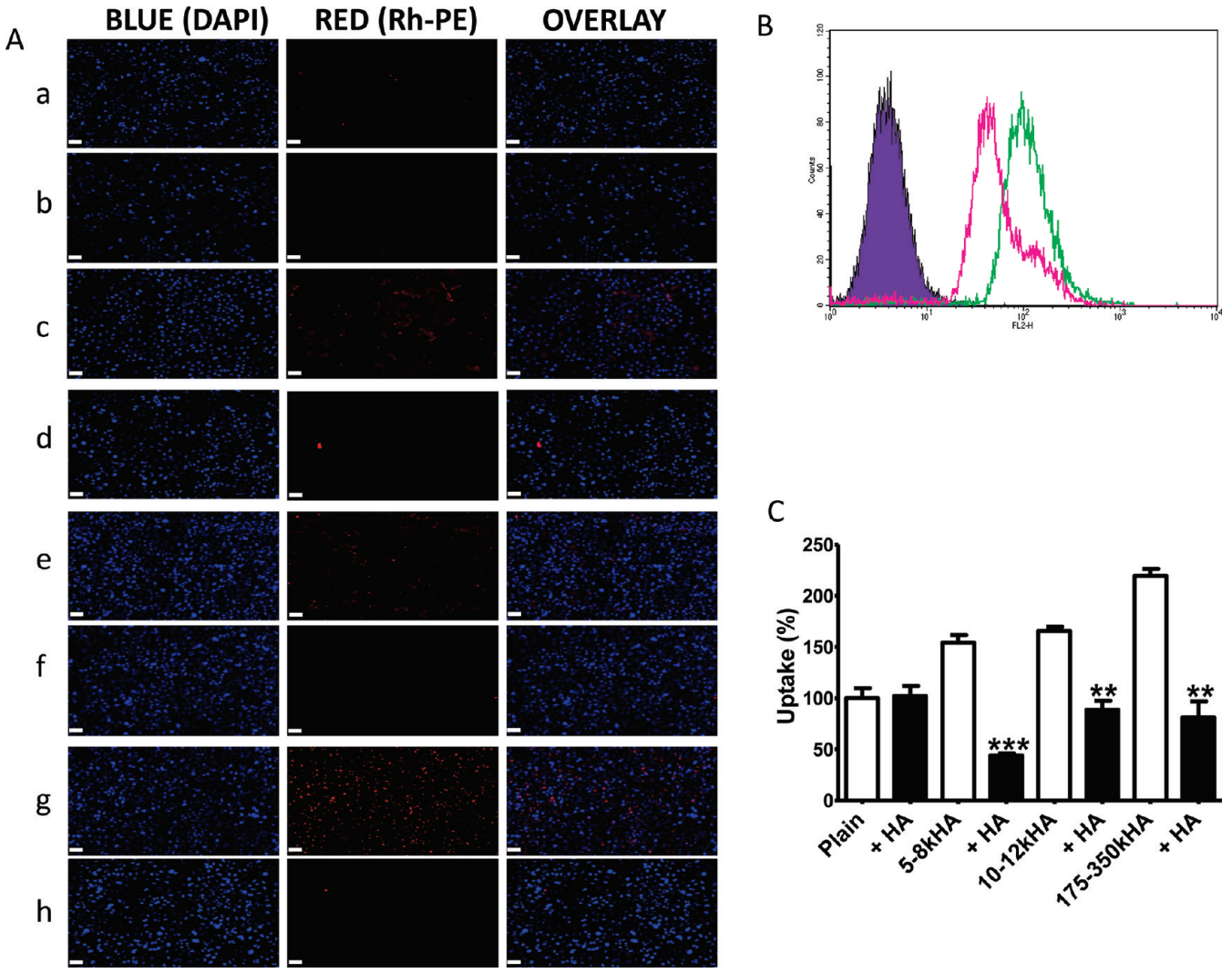

Figure 4. Effect of ligand pretreatment on cellular uptake of HA−liposomes in A549 cells. The A549 cells were preincubated with 175−350 kDa HA (10 mg/mL) for 1 h before the addition of various liposomes. (A) Fluorescence microscopy images display cellular association and uptake of Rh-PE labeled plain liposomes (a), plain liposomes after HA pretreatment (b), 5−8 kDa HA−liposomes (c), 5−8 kDa HA−liposomes after HA pretreatment (d), 10−12 kDa HA−liposomes (e), 10−12 kDa HA−liposomes after HA pretreatment (f), 175−350 kDa HA−liposomes (g), and 175−350 kDa HA−liposomes after HA pretreatment (h). The blue channel represents DAPI stained nuclei, the red channel represents the Rh-PE labeled liposomes, and the overlay represents cellular association of liposomes. Images are at 100× magnification, and scale bar is 50 μm. (B) The flow cytometry histogram displays the relative fluorescence intensity of unstained control A549 cells (filled curve) or cells treated with Nile Red loaded 5−8 kDa HA−liposomes with (red curve) and without HA pretreatment (green curve). (C) The quantitative analysis of percentage of cellular uptake of Nile Red labeled different molecular weights of HA−liposomes with or without HA pretreatment. The bars represent mean ± SEM of each treatment, $n = 3$, ** represents $p < 0.01$, *** represents $p < 0.001$ after Student's t-test.

confirmed in the MDA-MB-231 cells (Figure S2 in the Supporting Information). The quantitative flow cytometric analysis of Nile Red loaded liposomes showed that the mean fluorescence intensity of the liposomes conjugated to 175−350 kDa-HA was 30−40% higher than that of liposomes conjugated to lower molecular weight HA (5−8 or 10−12 kDa, $p < 0.0001$, one way ANOVA, Figure 3C) in A549 cells. We also determined concentration dependent binding and internalization of HA−liposomes in A549 cells. A statistically significant increase in binding and internalization of liposomes (plain <5−8 kDa HA−liposome <175−350 kDa HA−liposome) was observed when cells were treated with increasing concentrations of Nile Red loaded HA−liposomes (0.5−10 μM Nile Red, 0.1−2 mM total lipids, $p < 0.001$, two-way ANOVA, Figure 3D). These data suggest that the size of HA ligand is an important determinant of its cellular uptake, with higher MWs of HA resulting in better cellular adhesion and internalization of HA−liposomes.

Effect of HA Blocking on Cellular Uptake of HA−Liposomes. To further verify if the uptake of the HA−liposomes is specific to CD44 receptor, competitive binding experiments were performed by pretreating the A549 cells with a saturable amount of free HA (175−350 kDa) before HA−liposome incubation. Fluorescence microscopy studies revealed that the ligand pretreatment did not change the fluorescence intensities of Rh-PE labeled plain liposomes, but significantly diminished the red fluorescence of HA−liposomes (5−8, 10−12, and 175−350 kDa, Figure 4A), indicating that the free ligand competes with the HA−liposomes for receptor binding sites. Similar results were

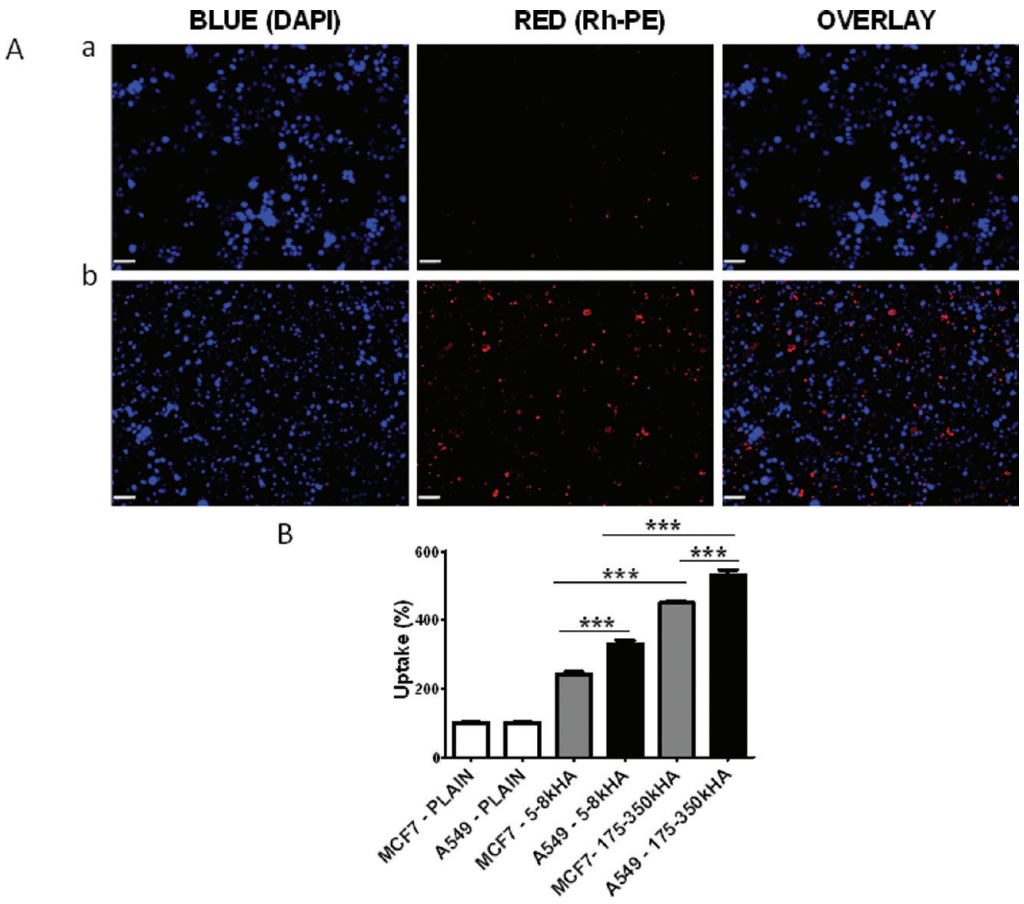

Figure 5. Cellular uptake of HA−liposomes in CD44 low and high expression cell lines. (A) Fluorescence microscopy images display cellular association and uptake of Rh-PE labeled 5−8 kDa HA−liposomes in MCF7 cells (low CD44 expression) (a), and A549 cells (high CD44 expression) (b). The blue channel shows DAPI stained nuclei, the red channel displays the red Rh-PE liposomes, and the overlay represents cellular association of liposomes. Images are at 100× magnification, and the scale bar is 50 μm. (B) The quantitative flow cytometry analysis of uptake of Nile Red labeled HA−liposomes in MCF7 and A549 cells where the uptake of plain liposomes in each cell line was set as 100%. Data is presented as mean ± SEM, $n = 3-6$, *** represents $p < 0.001$ after Student's *t*-test.

obtained in low CD44 expressing cells MCF7 (Figure S3 in the Supporting Information). Quantitative results were obtained by flow cytometry analysis (Figures 4B and 4C) where, compared to the uptake of control cells without HA pretreatment, the cells pretreated with excess ligand had nearly 50−70% reduction in mean fluorescence in all the Nile Red loaded HA (5−8, 10−12, and 175−350 kDa)-conjugated liposomes (Figure 4C, $p < 0.01$, Student's *t*-test). The ligand HA pretreatment had no effect on the uptake of Nile Red loaded plain liposomes (Figure 4C). These results suggest that the binding and internalization of these HA−liposomes to A549 cells could be competitively inhibited by excess free HA, demonstrating that the HA cell surface receptors, predominantly CD44 receptors, mediate the interaction.

Influence of CD44 Surface Density on Cellular Uptake of HA−Liposomes. To investigate whether the HA−liposome uptake was dependent on the cell surface expression level of CD44 receptor, we used MCF7 (CD44 low expression) and A549 (CD44 high expression) to determine if higher expression of CD44 receptor translates into higher uptake of HA−liposomes. Figure 5A showed that Rh-PE red fluorescence associated with 5−8 kDa HA−liposomes was lower in MCF7 cells in comparison to that of A549 cells. The quantitative flow cytometric analysis showed that the relative uptake of Nile Red loaded HA−liposomes (5−8 and 175−350 kDa) was significantly higher in A549 cells compared to MCF7 cells ($p < 0.001$, Student's *t*-test). These studies are in agreement with the CD44 receptor-mediated uptake of HA−liposomes because the targeting efficiency is dependent on the cell surface receptor density.

The Endocytic Pathway of HA−Liposomes. To further probe the intracellular transporting mechanism of these HA−liposomes, we studied the effects of temperature and several membrane entry inhibitors on cellular internalization of HA−liposomes. Extracellular materials are usually translocated across the cell membrane by endocytosis. We found that the incubation of HA−liposomes with cells at 4 °C, which inhibits all the active energy-mediated processes, reduces uptake of 5−8 kDa and 175−350 kDa HA−liposomes by 68% and 53%, respectively, compared to uptake at 37 °C. This finding indicates that HA−liposomes are taken up inside the cells via an energy-dependent endocytosis pathway.

To further elucidate the endocytic pathway, we used flow cytometry to study the effects of several membrane entry inhibitors on the cellular internalization of HA−liposomes (Figure 6). A549 cells were pretreated with individual inhibitors, at concentrations that were not cytotoxic to the cells, before incubation with 5−8 kDa and 175−350 kDa HA-conjugated liposomes. Cells treated in the absence of inhibitors were used as

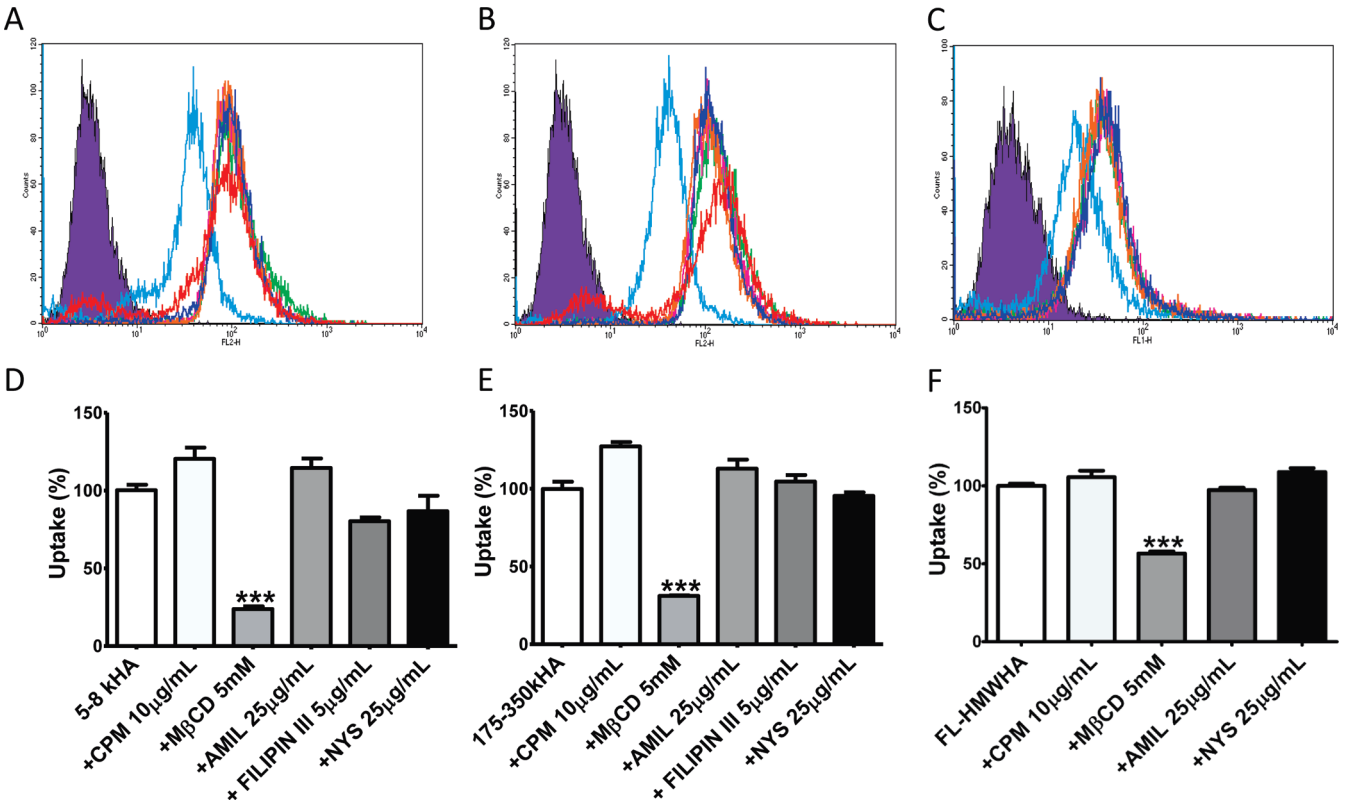

Figure 6. Effect of endocytosis inhibitors on cellular uptake of Nile Red labeled 5−8 kDa HA−liposomes (A, D), 175−350 kDa HA−liposomes (B, E), and fluorescein-labeled HMWHA (C, F). Flow cytometry histogram shows the fluorescence intensities of unstained A549 cells (filled curve) and cells treated with HA−liposomes (5−8, 175−350 kDa) or fluorescein-HMWHA without inhibitor pretreatment (green curve) or with chlorpromazine (CPM, 10 μg/mL, red curve) to inhibit clathrin-mediated endocytosis, methyl-β-cyclodextrin (MβCD, 5 mM, blue curve) to inhibit lipid raft-mediated endocytosis, amiloride (AMIL, 10 μg/mL, brown curve) to inhibit macropinocytosis, or filipin III (5 μg/mL, red curve) or nystatin (NYS, 25 μg/mL, dark blue curve) to inhibit caveolae-specific endocytosis. All inhibitors were preincubated for 1 h. The percentage of uptake was calculated based on the fluorescence intensity of cellular uptake without any pretreatment (100%) and is presented as mean ± SEM, $n = 3-6$, *** represents $p < 0.0001$ after one way ANOVA.

controls. Inhibition of clathrin-mediated uptake was tested by using chlorpromazine, which inhibits assembly and disassembly of clathrin.[37] Caveolae-mediated uptake was tested by filipin III and nystatin, which partition into membranes and sequester sterols.[38] Macropinocytosis, a mechanism that mainly contributes to antigen uptake by professional antigen-presenting cells, was tested by amiloride, a specific inhibitor of the Na^+/H^+ exchange required for macropinocytosis. None of these inhibitors showed any significant effects on the uptake of both HA−liposomes (Figure 6). These results suggest that the CD44-mediated internalization of HA−liposomes is independent of clathrin-coated vesicles or the caveolae or macropinocytosis pathways.

It has been reported that cholesterol and lipid rafts are involved in membrane trafficking.[39] Lipid rafts are plasma membrane microdomains rich in cholesterol, sphingolipids, and cell surface receptors. To examine the role of lipid rafts in the uptake of HA−liposomes, the A549 cells were treated with methyl-β-cyclodextrin (MβCD), a water-soluble cyclic glucopyranoside oligomer and an inhibitor of lipid rafts. MβCD can selectively deplete cholesterol and disrupt lipid rafts without being incorporated into the plasma membrane.[38,40] As compared to the controls, cells treated with MβCD showed significantly reduced uptake of both 5−8 kDa and 175−350 kDa HA−liposomes (Figure 6, $p < 0.0001$, one-way ANOVA). To confirm the role of lipid rafts, we further repeated the study with fluorescein-conjugated high molecular weight HA (~1600 kDa). Similar to the above results, the uptake of the fluorescent polymer was reduced by nearly 45% with MβCD pretreatment, compared to untreated cells (Figure 6C and 6F, $p < 0.0001$, one way ANOVA). These results suggest that HA−liposomes are taken up into the cells via the lipid raft-mediated endocytosis which is cholesterol-dependent and is inhibited by methyl-β-cyclodextrin pretreatment.

Cellular Localization of HA−Liposomes. To investigate the intracellular localization of HA−liposomes, we incubated the Rh-PE labeled plain liposomes or HA−liposomes with A549 cells for 2 h and monitored internalization using fluorescence microscopy. We used LysoTracker Green (a cell-permeable weakly basic amine) to stain for the acidic compartments (endosomal and lysosomal vesicles) and DAPI to label the nucleus (Figure 7A). The red fluorescence from liposomes (Figure 7B) and green fluorescence from LysoTracker (Figure 7C) were then visualized. We observed that the 175−350 kDa HA−liposomes mainly localized in acidic compartments such as endosomal and lysosomal vesicles, as evidenced by colocalization of green and red fluorescence (Figure 7D, 7E). The magnified image of colocalization showed that Rh-PE labeled HA−liposomes produced a very bright, punctuated pattern (red dots, Figure S4 in the Supporting Information) and a fraction of HA−liposomes colocalized with LysoTracker Green. A smaller fraction of

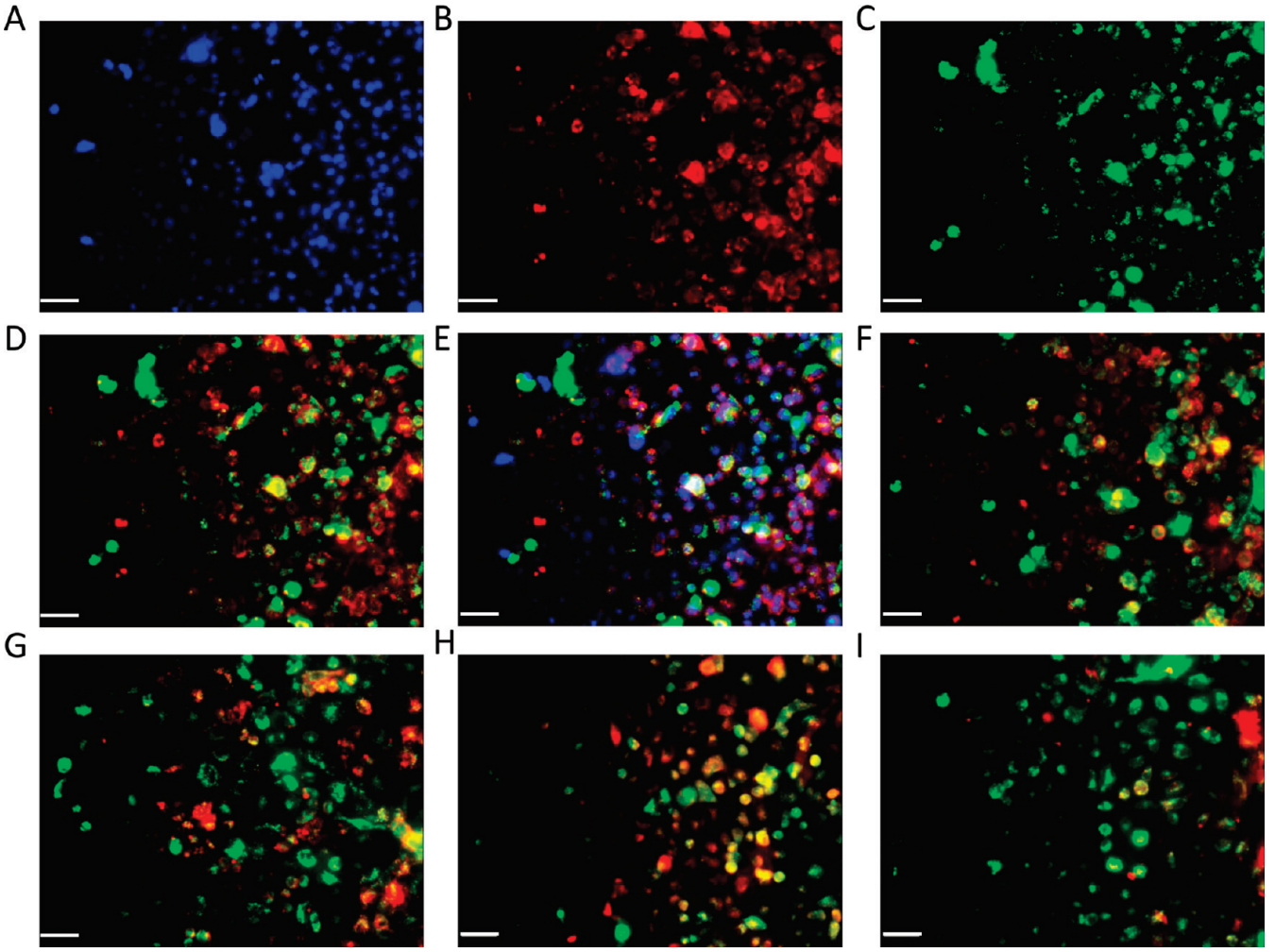

Figure 7. Localization and distribution of plain liposomes or HA−liposomes in A549 cells. Cells were incubated with Rh-PE labeled 175−350 kDa HA−liposomes for 2 h at 37 °C before fluorescence microscopy analysis. Blue fluorescence represents DAPI stained nuclei (A), red fluorescence represents the Rh-PE labeled liposomes (B), green fluorescence represents acidic compartments of endosomes and lysosomes (C). Yellow color observed in the red + green overlay (D) is due to the colocalization of red liposomes with the green endosomes and lysosomes. The blue + green + red overlay (E) represents cellular association and intracellular localization of HA−liposomes. The red + green overlays display localization of endosomes and lysosomes with 5−8 kDa HA−liposomes (F), plain liposomes (G), Texas Red dextran 3 kDa (H), or Texas Red-HA 5−8 kDa (I). Images are at 320× magnification, and the scale bar is 25 μm.

5−8 kDa HA−liposomes (Figure 7F) and plain liposomes (Figure 7G) also displayed partial colocalization with the LysoTracker Green after 2 h of incubation. To further confirm the results, Texas Red labeled 3 kDa dextran, a probe known for labeling the lysosomal compartment,[41] was used as a positive control for lysosomal localization. As expected, Texas Red 3 kDa dextran was completely colocalized with the LysoTracker Green staining (Figure 7H). Additionally, we observed the colocalization of Texas Red conjugated 5−8 kDa HA with the LysoTracker Green (Figure 7I), which is consistent with the literature data indicating that free HA mainly resides in prelysosomal endosomes.[34] Taken together, these experiments suggest that the HA−liposomes are predominantly localized in acidic endosome and lysosome compartments.

DISCUSSION

Hyaluronan has been used as a drug carrier and a ligand on liposomal NP to actively target tumor cells.[9] High molecular weight HA was attached to liposomes as a bioadhesive formulation to adhere to the extracellular matrix for topical delivery.[42] Further, Peer et al. encapsulated anticancer drugs mitomycin C or doxorubicin into the HA−liposome (HMWHA, ~10^6 Da), which had a half-life slightly less than that of PEGylated "stealth" liposome and improved survival time in multiple cancer models.[26,43] In another work, Szoka et al. attached a mixture of oligosaccharide HA (tetramer/hexamer/octamer) to PE lipid directly before liposome preparation and encapsulated doxorubicin to the oligo HA−liposomes (HAL-DOX). The HAL-DOX exhibited 8.2- or 4.4-fold increase in potency, compared with the free doxorubicin, against the B16F10 melanoma cells in a transient-exposure or continuous-exposure condition, respectively.[27] Moreover, large molecular weight HA-coated liposomes have been used recently for delivery of RNAi payloads[44,45] or MRI contrast agents.[46] These data suggest that HA conjugation of DDS could potentially improve the delivery and effectiveness of anticancer drugs.

The above reports established the advantages of HA−liposomes over nontargeted delivery systems. However, the effects of

HA size and density on the delivery system−CD44 interaction in target cells of varying CD44 expression levels and the mechanisms of the HA−liposome intracellular trafficking are largely unknown. The HA−CD44 interactions and intracellular trafficking of the DDS affect the specific delivery of the cargo and its downstream effects, such as toxicity and pharmacodynamics. In the current study we have addressed these important issues, which are crucial for the rational design and optimization of CD44-targeted, hyaluronan-based nanotherapeutics for improved intracellular delivery.

The large molecular weight HA-coated liposomes were shown to improve cell uptake in A549[47] and MDA-MB-231 cells but not in MCF7 cells,[48] Our results confirmed the high expression of CD44 receptors in A549 and MDA-MB-231 cells, and low expression of CD44 in MCF7 cells. Furthermore, our results showed strong expression of surface CD44 receptor as compared to surface CD168 receptor in all cells, indicating that CD44, not CD168, is the principal HA receptor for mediating cellular uptake of HA-coated liposomes (Figure 1A). For MDA-MB-231 cells, a low level of CD168 receptor was observed, suggesting CD168 may make a minor contribution to cellular uptake of HA−liposome in MDA-MB-231 cells. We did not study other hyaluronan receptors, because HARE receptor is mainly expressed in sinusoidal endothelial cells,[14] and Toll-like receptors-2 and -4 are mainly expressed in immune cells.[15]

For ligand-targeted nanoparticle DDS, tuning the surface ligand density (for enhanced ligand coverage) is a key requirement for efficient cellular targeting and preferential drug delivery to malignant sites. The quantity of the surface anchored HA was not measured in previous studies. In the current study, we characterized the amount of HA conjugated on the surface of liposomes using the CTAB turbidimetric method. We observed that there was a minimum threshold of HA ligand grafting density that is required, above which efficient uptake of HA−liposomes via the CD44 receptor occurs (Figure 2E). In addition to HA density, our results (Figure 5) demonstrate that the degree of intracellular uptake of HA−liposomes also depends on the receptor density of the cells; higher CD44 receptor density correlates with higher HA−liposome uptakes. This property makes the HA−liposome DDS system tumor-selective because many tumor cells overexpress CD44 receptor, which advantageously leads to improved HA−liposome uptake. On the other hand, the normal cells with no or relatively low CD44 receptors will be minimally affected by the HA-targeted nanocarrier systems.

Our results (Figure 2A) suggest that the physicochemical properties of the HA−liposomes are affected by the MW of the HA. We observed a trend that mean particle sizes of the negatively charged HA−liposomes progressively increased with an increase in the MW of HA (Figure 2A). This is in agreement with the reported change in hydrodynamic radius of HA as a result of chain length; the hydrodynamic radius of HA polymer increases from 22 nm at 160 kDa to 36 nm at 350 kDa, to 56 nm at 800 kDa, to 81 nm at 1430 kDa.[49] Additionally, the MW of HA affected the charge of the HA−liposome. Generally, as the MW of HA increased from 5−8 kDa to 1600 kDa, there was a substantial increase in the zeta potential of the nanoparticle (Figure 2A). However, this relationship is not very clear if only the 5−8 kDa and 10−12 kDa HA−liposomes are considered (Figure 2A), perhaps because of the low and variable charge at this MW range (Figure 2A). Nevertheless, the relationship between the polymer MW and charge may be complicated by other factors affecting the measurement of surface charge. For example, the surface charge can be influenced by the HA conformation adopted (e.g., fully relaxed chain, densely packed coils, or short thick rod), intermolecular hydrogen bonding between the carboxyl group and acetamido group, or surface interaction with lipids. Overall, these data suggest that the MW of HA contributes to both the size and charge of the HA−liposomes.

In previous studies of HA−liposomes, the HAs used were highly heterogeneous with respect to size. Because of different binding affinity and opposing biological effects with HMWHA and LMWHA, HA of defined molecular weight was used in the current study. The binding affinity of fluorescein-labeled HA to CD44 receptor increased with increasing size of HA (5−8 ≈ 10−12 < 175−350 < 1600 kDa) in all cell lines (Figure 3A, Figure S1 in the Supporting Information). However, similar to previous observations,[35] the difference of binding affinity of LMWHA 5−8 and 10−12 kDa to CD44 receptor was not clearly detected by flow cytometry. Our results are consistent with earlier studies using ^{3}H-HA radioligand binding assay that showed high MW of HA had a higher binding affinity to SV-3T3 (simian virus 40-transformed Swiss mouse 3T3) cells than did smaller MW of HA, with dissociation constant (K_d) values of 3.4×10^{-9} M for the 4.5×10^{5} Da HA, 2.01×10^{-9} M for the 9.2×10^{5} Da HA, and 1.47×10^{-9} M for the 1.3×10^{6} Da HA.[50] The hyaluronan receptor in SV-3T3 cell was later proved to be CD44.[51] Similarly, the binding of ^{125}I-Tyr labeled HA (4.5×10^{5} Da) on a rat colon cancer cell line was competitively inhibited more effectively by HMWHA than LMWHA, with a K_d value of 1.4×10^{-9} M.[52] Additionally, the size-dependence of ^{3}H-HA binding to liver endothelial cells was also demonstrated by a preference of cell surface binding for HMWHA; the dissociation constant decreased dramatically with an increasing size of HA, with K_d values of 4.6×10^{-6} M for an octasaccharide HA, 0.2×10^{-6} M for HA of 35 sugar residues, 6×10^{-11} M for the 4×10^{5} Da HA, and 9×10^{-12} M for the 6.4×10^{6} Da HA.[53] A minimal binding site size of six sugar residues is required for HA binding to cell surface CD44.[35] This information indicates that the importance of molecular weight of HA in determining the its cellular binding efficiency.

This molecular weight dependency was also observed in HA-coated liposomes. Increasing the MW of HA from 5−8 kDa to 175−350 kDa enhances the uptake of HA−liposomes (Figures 3 and 5). This could be attributed to a higher binding affinity of high molecular weight HA to CD44 receptor, compared to low molecular weight HA (Figure 3A).[35] In addition, the longer polymeric chains of HA extending from the liposome surface improve ligand accessibility to the CD44 receptor and promote the multivalent binding to receptor. Our results are consistent with a recent study[24] on the free flexible HA polymer binding and adsorption on an adhesive surface coated with CD44, which showed that the binding of high molecular weight HA (>262 kDa) was irreversible. However, the binding became weaker and reversible with decreased HA molecular weight.[24]

We demonstrated that the maximum HA−liposome−CD44 receptor binding effect can be achieved by increasing either HA chain length (Figure 3) or grafting density (Figure 2E). However, an inherent disadvantage of HMWHA as a polymer excipient is that it is quickly cleared from circulation by the liver and spleen.[54−56] Additionally, increasing the size of HA also increases the inherent viscosity of HA polymer, making the HA−liposomes sticky and separation of unconjugated HMWHA from HA−liposome preparations is not efficient. Free HMWHA may

compete with the HA−liposomes for receptor binding sites and hamper the uptake of HA−liposomes. Therefore, 1600 kDa HMWHA may not be an ideal ligand for coating liposomes despite its high receptor binding affinity. The optimal size of HA for construction of tumor-targeted HA−liposomes will have to balance the receptor affinity, circulation half-life, and tumor/liver accumulation ratios. In principle, linear HA polymer can behave just like PEG. This means, depending on the size of HA and grafting density, HA chains grafted on the lipid bilayers can show brush, mushroom, or pancake conformation. Each conformation has different thickness of hydration layer and different steric hindrance.[57] All of these could potentially affect circulation half-life. Shorter polymer chain length may have longer circulation, as PEG_{5000} liposomes show similar or even reduced circulation times compared to PEG_{2000} liposomes at similar lipid-to-polymer mole ratios.[58] Nevertheless, our results indicate that both the HA MW and grafting density should be tuned to be effective by either high affinity ligand or high density of multiple ligands with moderate affinity. Future studies of the biodistribution and intratumoral accumulation of different MWs of HA−liposomes in tumor-bearing animal models will allow selecting HA−liposome with optimized pharmacokinetics and tumor targeting properties.

Cells use endocytosis as a tool to internalize a variety of cargos. The receptor-mediated endocytosis is a complex and highly regulated process, which involves the binding, internalization, and transfer of ligands through a series of distinct intracellular compartments. A recent report[59] showed that the endocytic patternings of anti-EGFR antibody C225 and gold-conjugated C225 nanoparticles were different. Thus, the nanoconjugation may potentially alter and modulate the endocytic pathways.[59] The mechanism and pattern of free HA polymer-induced endocytosis is still not fully understood.[34] Indeed, some have even argued that the mammalian endocytic HA receptor is HARE instead of CD44.[14,60,61] Furthermore, it is unknown whether nanoconjugation could lead to the alteration of the mechanism of endocytosis of HA−liposomes.

In the current study, we observed that the CD44-mediated internalization of HA−liposomes occurs via the lipid raft-mediated endocytosis pathway and is independent of clathrin-coated vesicles or the caveolae or macropinocytosis pathways (Figure 6). Lipid rafts are dynamic assemblies in cell membranes enriched in cholesterol and sphingolipids such as sphingomyelin and gangliosides.[62] These specialized membrane microdomains exhibit more ordered and tightly packed bilayers and float freely in the plasma membrane. Lipid rafts serve as a platform for assembly of signaling molecules, eliciting controlled signal transduction, and influencing membrane protein and cellular receptor trafficking.[39,62,63] Previous studies showed that CD44 localizes in detergent-resistant cholesterol-rich lipid rafts[64] and associates directly or indirectly with signaling proteins and transporters.[65−67] Both HMWHA and LMWHA can rapidly recruit CD44s to the lipid raft fraction.[68] Moreover, recent reports show that disintegration of membrane lipid rafts by MβCD enhances CD44 shedding.[67] Our results (Figure 6) indicate that, similar to free HA polymer, HA−liposomes are taken up via lipid raft-mediated endocytosis, which is energy and cholesterol dependent. Depletion of cholesterol by MβCD could potentially lead to shedding of CD44 receptors in the lipid raft and result in the reduced HA−liposome uptake, as observed in our studies (Figure 6).

We have demonstrated that a fraction of the endocytosed HA−liposomes resides in low pH intracellular compartments such as endolysosomal vesicles (Figure 7). This is consistent with published data showing that free HA resides in prelysosomal endosomes.[34] Intracellular trafficking of HA−liposomes is a highly dynamic process as receptor CD44 rapidly recycles from the intracellular compartment to the plasma membrane. The intracellular fate of HA−liposomes will impact the specific delivery and release of cargos and elicit downstream pharmacodynamic effect.

In summary, the maximum HA−liposome−CD44 receptor binding effect can be achieved by increasing either HA chain length or grafting density. HA−liposomes mainly reside in low pH intracellular compartments. Fine tuning the HA molecular weight and grafting density will optimize the HA−liposomes for improved intratumoral delivery. This information is crucial for the design of optimal formulations for the *in vivo* delivery of anticancer therapeutics using hyaluronan-conjugated delivery systems.

■ ASSOCIATED CONTENT

Supporting Information. FL-HA binding with MDA-MB-231 and MCF7 cells, fluorescence microscopy images of Rh-PE labeled liposomes in MDA-MB-231 and MCF7 cells, and cellular colocalization images of Rh-PE labeled liposomes and LysoTracker Green in A549 cells. This material is available free of charge via the Internet at http://pubs.acs.org.

■ AUTHOR INFORMATION

Corresponding Author

*Department of Pharmaceutical Sciences, School of Pharmacy, Texas Tech University Health Sciences Center, 1406 Coulter Drive, Suite 1105, Amarillo, TX 79106. Phone: 806-356-4750 ext 226. Fax: 806-356-4770. E-mail: xinli.liu@ttuhsc.edu.

■ ACKNOWLEDGMENT

This work was funded in part by an NIH CTSA NCTCTSI Pilot award grant (UL1 RR024982) and a Laura W. Bush Institute for Women's Health seed grant. The technical support of Liangxi Li, Rajendar Mittapalli, and Xiaolei Wang from TTUHSC is greatly appreciated. We thank Dr. Reza Mehvar from TTUHSC for critically reading the manuscript.

■ REFERENCES

(1) Brigger, I.; Dubernet, C.; Couvreur, P. Nanoparticles in cancer therapy and diagnosis. *Adv. Drug Delivery Rev.* **2002**, *54* (5), 631–51.

(2) Maeda, H.; Wu, J.; Sawa, T.; Matsumura, Y.; Hori, K. Tumor vascular permeability and the EPR effect in macromolecular therapeutics: a review. *J. Controlled Release* **2000**, *65* (1−2), 271–84.

(3) Matsumura, Y.; Maeda, H. A new concept for macromolecular therapeutics in cancer chemotherapy: mechanism of tumoritropic accumulation of proteins and the antitumor agent smancs. *Cancer Res.* **1986**, *46* (12 Part 1), 6387–92.

(4) Torchilin, V. P. Recent advances with liposomes as pharmaceutical carriers. *Nat. Rev. Drug Discovery* **2005**, *4* (2), 145–60.

(5) Allen, T. M. Ligand-targeted therapeutics in anticancer therapy. *Nat. Rev. Cancer* **2002**, *2* (10), 750–63.

(6) Ponta, H.; Sherman, L.; Herrlich, P. A. CD44: from adhesion molecules to signalling regulators. *Nat. Rev. Mol. Cell Biol.* **2003**, *4* (1), 33–45.

(7) Naor, D.; Sionov, R. V.; Ish-Shalom, D. CD44: structure, function, and association with the malignant process. *Adv. Cancer Res.* **1997**, *71*, 241–319.

(8) Visvader, J. E.; Lindeman, G. J. Cancer stem cells in solid tumours: accumulating evidence and unresolved questions. *Nat. Rev. Cancer* **2008**, *8* (10), 755–68.

(9) Platt, V. M.; Szoka, F. C., Jr. Anticancer therapeutics: targeting macromolecules and nanocarriers to hyaluronan or CD44, a hyaluronan receptor. *Mol. Pharmaceutics* **2008**, *5* (4), 474–86.
(10) Toole, B. P. Hyaluronan: from extracellular glue to pericellular cue. *Nat. Rev. Cancer* **2004**, *4* (7), 528–39.
(11) Scott, J. E.; Heatley, F. Hyaluronan forms specific stable tertiary structures in aqueous solution: a 13C NMR study. *Proc. Natl. Acad. Sci. U.S.A.* **1999**, *96* (9), 4850–5.
(12) Toole, B. P. Hyaluronan-CD44 Interactions in Cancer: Paradoxes and Possibilities. *Clin. Cancer Res.* **2009**, *15* (24), 7462–7468.
(13) Maxwell, C. A.; McCarthy, J.; Turley, E. Cell-surface and mitotic-spindle RHAMM: moonlighting or dual oncogenic functions? *J. Cell Sci.* **2008**, *121* (Part 7), 925–32.
(14) Zhou, B.; Weigel, J. A.; Saxena, A.; Weigel, P. H. Molecular cloning and functional expression of the rat 175-kDa hyaluronan receptor for endocytosis. *Mol. Biol. Cell* **2002**, *13* (8), 2853–68.
(15) Scheibner, K. A.; Lutz, M. A.; Boodoo, S.; Fenton, M. J.; Powell, J. D.; Horton, M. R. Hyaluronan fragments act as an endogenous danger signal by engaging TLR2. *J. Immunol.* **2006**, *177* (2), 1272–81.
(16) Harada, H.; Takahashi, M. CD44-dependent intracellular and extracellular catabolism of hyaluronic acid by hyaluronidase-1 and -2. *J. Biol. Chem.* **2007**, *282* (8), 5597–607.
(17) Noble, P. W. Hyaluronan and its catabolic products in tissue injury and repair. *Matrix Biol.* **2002**, *21* (1), 25–9.
(18) Gao, F.; Yang, C. X.; Mo, W.; Liu, Y. W.; He, Y. Q. Hyaluronan oligosaccharides are potential stimulators to angiogenesis via RHAMM mediated signal pathway in wound healing. *Clin. Invest. Med.* **2008**, *31* (3), E106–16.
(19) Deed, R.; Rooney, P.; Kumar, P.; Norton, J. D.; Smith, J.; Freemont, A. J.; Kumar, S. Early-response gene signalling is induced by angiogenic oligosaccharides of hyaluronan in endothelial cells. Inhibition by non-angiogenic, high-molecular-weight hyaluronan. *Int. J. Cancer* **1997**, *71* (2), 251–6.
(20) Bollyky, P. L.; Falk, B. A.; Wu, R. P.; Buckner, J. H.; Wight, T. N.; Nepom, G. T. Intact extracellular matrix and the maintenance of immune tolerance: high molecular weight hyaluronan promotes persistence of induced CD4+CD25+ regulatory T cells. *J. Leukocyte Biol.* **2009**, *86* (3), 567–72.
(21) Arnold, F.; Jia, C.; He, C.; Cherry, G. W.; Carbow, B.; Meyer-Ingold, W.; Bader, D.; West, D. C. Hyaluronan, heterogeneity, and healing: the effects of ultrapure hyaluronan of defined molecular size on the repair of full-thickness pig skin wounds. *Wound Repair Regener.* **1995**, *3* (3), 299–310.
(22) Svanovsky, E.; Velebny, V.; Laznickova, A.; Laznicek, M. The effect of molecular weight on the biodistribution of hyaluronic acid radiolabeled with 111In after intravenous administration to rats. *Eur. J. Drug Metab. Pharmacokinet.* **2008**, *33* (3), 149–57.
(23) Hisada, N.; Satsu, H.; Mori, A.; Totsuka, M.; Kamei, J.; Nozawa, T.; Shimizu, M. Low-molecular-weight hyaluronan permeates through human intestinal Caco-2 cell monolayers via the paracellular pathway. *Biosci., Biotechnol., Biochem.* **2008**, *72* (4), 1111–4.
(24) Wolny, P. M.; Banerji, S.; Gounou, C.; Brisson, A. R.; Day, A. J.; Jackson, D. G.; Richter, R. P. Analysis of CD44-hyaluronan interactions in an artificial membrane system: insights into the distinct binding properties of high and low molecular weight hyaluronan. *J. Biol. Chem.* **2010**, *285* (39), 30170–80.
(25) Yerushalmi, N.; Arad, A.; Margalit, R. Molecular and cellular studies of hyaluronic acid-modified liposomes as bioadhesive carriers for topical drug delivery in wound healing. *Arch. Biochem. Biophys.* **1994**, *313* (2), 267–73.
(26) Peer, D.; Margalit, R. Loading mitomycin C inside long circulating hyaluronan targeted nano-liposomes increases its antitumor activity in three mice tumor models. *Int. J. Cancer* **2004**, *108* (5), 780–9.
(27) Eliaz, R. E.; Szoka, F. C., Jr. Liposome-encapsulated doxorubicin targeted to CD44: a strategy to kill CD44-overexpressing tumor cells. *Cancer Res.* **2001**, *61* (6), 2592–601.
(28) de Belder, A. N.; Wik, K. O. Preparation and properties of fluorescein-labelled hyaluronate. *Carbohydr. Res.* **1975**, *44* (2), 251–7.
(29) Collis, L.; Hall, C.; Lange, L.; Ziebell, M.; Prestwich, R.; Turley, E. A. Rapid hyaluronan uptake is associated with enhanced motility: implications for an intracellular mode of action. *FEBS Lett.* **1998**, *440* (3), 444–9.
(30) Song, J. M.; Im, J. H.; Kang, J. H.; Kang, D. J. A simple method for hyaluronic acid quantification in culture broth. *Carbohydr. Polym.* **2009**, *78* (3), 633–634.
(31) Huang, M.; Ma, Z.; Khor, E.; Lim, L. Y. Uptake of FITC-chitosan nanoparticles by A549 cells. *Pharm. Res.* **2002**, *19* (10), 1488–94.
(32) Huth, U. S.; Schubert, R.; Peschka-Suss, R. Investigating the uptake and intracellular fate of pH-sensitive liposomes by flow cytometry and spectral bio-imaging. *J. Controlled Release* **2006**, *110* (3), 490–504.
(33) Ivanov, A. I. Pharmacological inhibition of endocytic pathways: is it specific enough to be useful? *Methods Mol. Biol.* **2008**, *440*, 15–33.
(34) Tammi, R.; Rilla, K.; Pienimaki, J. P.; MacCallum, D. K.; Hogg, M.; Luukkonen, M.; Hascall, V. C.; Tammi, M. Hyaluronan enters keratinocytes by a novel endocytic route for catabolism. *J. Biol. Chem.* **2001**, *276* (37), 35111–22.
(35) Lesley, J.; Hascall, V. C.; Tammi, M.; Hyman, R. Hyaluronan binding by cell surface CD44. *J. Biol. Chem.* **2000**, *275* (35), 26967–75.
(36) English, N. M.; Lesley, J. F.; Hyman, R. Site-specific de-N-glycosylation of CD44 can activate hyaluronan binding, and CD44 activation states show distinct threshold densities for hyaluronan binding. *Cancer Res.* **1998**, *58* (16), 3736–42.
(37) Wang, L. H.; Rothberg, K. G.; Anderson, R. G. Mis-assembly of clathrin lattices on endosomes reveals a regulatory switch for coated pit formation. *J. Cell Biol.* **1993**, *123* (5), 1107–17.
(38) Brown, D. A. Lipid rafts, detergent-resistant membranes, and raft targeting signals. *Physiology (Bethesda)* **2006**, *21*, 430–9.
(39) Simons, K.; Ikonen, E. Functional rafts in cell membranes. *Nature* **1997**, *387* (6633), 569–72.
(40) Manunta, M.; Tan, P. H.; Sagoo, P.; Kashefi, K.; George, A. J. Gene delivery by dendrimers operates via a cholesterol dependent pathway. *Nucleic Acids Res.* **2004**, *32* (9), 2730–9.
(41) Boonen, M.; Hamer, I.; Boussac, M.; Delsaute, A. F.; Flamion, B.; Garin, J.; Jadot, M. Intracellular localization of p40, a protein identified in a preparation of lysosomal membranes. *Biochem. J.* **2006**, *395* (1), 39–47.
(42) Yerushalmi, N.; Margalit, R. Hyaluronic acid-modified bioadhesive liposomes as local drug depots: effects of cellular and fluid dynamics on liposome retention at target sites. *Arch. Biochem. Biophys.* **1998**, *349* (1), 21–6.
(43) Peer, D.; Margalit, R. Tumor-targeted hyaluronan nanoliposomes increase the antitumor activity of liposomal Doxorubicin in syngeneic and human xenograft mouse tumor models. *Neoplasia* **2004**, *6* (4), 343–53.
(44) Chono, S.; Li, S. D.; Conwell, C. C.; Huang, L. An efficient and low immunostimulatory nanoparticle formulation for systemic siRNA delivery to the tumor. *J. Controlled Release* **2008**, *131* (1), 64–9.
(45) Peer, D.; Park, E. J.; Morishita, Y.; Carman, C. V.; Shimaoka, M. Systemic leukocyte-directed siRNA delivery revealing cyclin D1 as an anti-inflammatory target. *Science* **2008**, *319* (5863), 627–30.
(46) Esposito, G.; Geninatti Crich, S.; Aime, S. Efficient cellular labeling by CD44 receptor-mediated uptake of cationic liposomes functionalized with hyaluronic acid and loaded with MRI contrast agents. *ChemMedChem* **2008**, *3* (12), 1858–62.
(47) Taetz, S.; Bochot, A.; Surace, C.; Arpicco, S.; Renoir, J. M.; Schaefer, U. F.; Marsaud, V.; Kerdine-Roemer, S.; Lehr, C. M.; Fattal, E. Hyaluronic acid-modified DOTAP/DOPE liposomes for the targeted delivery of anti-telomerase siRNA to CD44-expressing lung cancer cells. *Oligonucleotides* **2009**, *19* (2), 103–16.
(48) Surace, C.; Arpicco, S.; Dufay-Wojcicki, A.; Marsaud, V.; Bouclier, C.; Clay, D.; Cattel, L.; Renoir, J. M.; Fattal, E. Lipoplexes targeting the CD44 hyaluronic acid receptor for efficient transfection of breast cancer cells. *Mol. Pharmaceutics* **2009**, *6* (4), 1062–73.
(49) La Gatta, A.; De Rosa, M.; Marzaioli, I.; Busico, T.; Schiraldi, C. A complete hyaluronan hydrodynamic characterization using a size exclusion chromatography-triple detector array system during in vitro enzymatic degradation. *Anal. Biochem.* **2010**, *404* (1), 21–9.

(50) Underhill, C. B.; Toole, B. P. Physical characteristics of hyaluronate binding to the surface of simian virus 40-transformed 3T3 cells. *J. Biol. Chem.* **1980**, *255* (10), 4544–9.

(51) Culty, M.; Miyake, K.; Kincade, P. W.; Sikorski, E.; Butcher, E. C.; Underhill, C. The hyaluronate receptor is a member of the CD44 (H-CAM) family of cell surface glycoproteins. *J. Cell Biol.* **1990**, *111* (6 Part 1), 2765–74.

(52) Samuelsson, C.; Gustafson, S. Studies on the interaction between hyaluronan and a rat colon cancer cell line. *Glycoconjugate J.* **1998**, *15* (2), 169–75.

(53) Laurent, T. C.; Fraser, J. R.; Pertoft, H.; Smedsrod, B. Binding of hyaluronate and chondroitin sulphate to liver endothelial cells. *Biochem. J.* **1986**, *234* (3), 653–8.

(54) Coradini, D.; Zorzet, S.; Rossin, R.; Scarlata, I.; Pellizzaro, C.; Turrin, C.; Bello, M.; Cantoni, S.; Speranza, A.; Sava, G.; Mazzi, U.; Perbellini, A. Inhibition of hepatocellular carcinomas in vitro and hepatic metastases in vivo in mice by the histone deacetylase inhibitor HA-But. *Clin. Cancer Res.* **2004**, *10* (14), 4822–30.

(55) Fraser, J. R.; Dahl, L. B.; Kimpton, W. G.; Cahill, R. N.; Brown, T. J.; Vakakis, N. Elimination and subsequent metabolism of circulating hyaluronic acid in the fetus. *J. Dev. Physiol.* **1989**, *11* (4), 235–42.

(56) Sugahara, S.; Okuno, S.; Yano, T.; Hamana, H.; Inoue, K. Characteristics of tissue distribution of various polysaccharides as drug carriers: influences of molecular weight and anionic charge on tumor targeting. *Biol. Pharm. Bull.* **2001**, *24* (5), 535–43.

(57) Čeh, B.; Winterhalter, M.; Frederik, P. M.; Vallner, J. J.; Lasic, D. D. Stealth® liposomes: From theory to product. *Adv. Drug Delivery Rev.* **1997**, *24* (2−3), 165–177.

(58) Allen, T. M.; Hansen, C.; Martin, F.; Redemann, C.; Yau-Young, A. Liposomes containing synthetic lipid derivatives of poly-(ethylene glycol) show prolonged circulation half-lives in vivo. *Biochim. Biophys. Acta* **1991**, *1066* (1), 29–36.

(59) Bhattacharyya, S.; Bhattacharya, R.; Curley, S.; McNiven, M. A.; Mukherjee, P. Nanoconjugation modulates the trafficking and mechanism of antibody induced receptor endocytosis. *Proc. Natl. Acad. Sci. U.S. A.* **2010**, *107* (33), 14541–6.

(60) Weigel, J. A.; Raymond, R. C.; Weigel, P. H. The hyaluronan receptor for endocytosis (HARE) is not CD44 or CD54 (ICAM-1). *Biochem. Biophys. Res. Commun.* **2002**, *294* (4), 918–22.

(61) Weigel, J. A.; Weigel, P. H. Characterization of the recombinant rat 175-kDa hyaluronan receptor for endocytosis (HARE). *J. Biol. Chem.* **2003**, *278* (44), 42802–11.

(62) Simons, K.; Gerl, M. J. Revitalizing membrane rafts: new tools and insights. *Nat. Rev. Mol. Cell Biol.* **2010**, *11* (10), 688–99.

(63) Pike, L. J. Rafts defined: a report on the Keystone Symposium on Lipid Rafts and Cell Function. *J. Lipid Res.* **2006**, *47* (7), 1597–8.

(64) Oliferenko, S.; Paiha, K.; Harder, T.; Gerke, V.; Schwarzler, C.; Schwarz, H.; Beug, H.; Gunthert, U.; Huber, L. A. Analysis of CD44-containing lipid rafts: Recruitment of annexin II and stabilization by the actin cytoskeleton. *J. Cell Biol.* **1999**, *146* (4), 843–54.

(65) Bourguignon, L. Y.; Singleton, P. A.; Diedrich, F.; Stern, R.; Gilad, E. CD44 interaction with Na+-H+ exchanger (NHE1) creates acidic microenvironments leading to hyaluronidase-2 and cathepsin B activation and breast tumor cell invasion. *J. Biol. Chem.* **2004**, *279* (26), 26991–7007.

(66) Lee, J. L.; Wang, M. J.; Sudhir, P. R.; Chen, J. Y. CD44 engagement promotes matrix-derived survival through the CD44-SRC-integrin axis in lipid rafts. *Mol. Cell. Biol.* **2008**, *28* (18), 5710–23.

(67) Murai, T.; Maruyama, Y.; Mio, K.; Nishiyama, H.; Suga, M.; Sato, C. Low cholesterol triggers membrane microdomain-dependent CD44 shedding and suppresses tumor cell migration. *J. Biol. Chem.* **2010**.

(68) Singleton, P. A.; Dudek, S. M.; Ma, S. F.; Garcia, J. G. Transactivation of sphingosine 1-phosphate receptors is essential for vascular barrier regulation. Novel role for hyaluronan and CD44 receptor family. *J. Biol. Chem.* **2006**, *281* (45), 34381–93.